Multi-Order Dynamic Range DNA Sensor Using a Gold Decorated SWCNT Random Network

Jung Woo Ko,[†,‡,⊥] Jun-Myung Woo,[§,⊥] Jinhong Ahn ,[†,⊥] Jun Ho Cheon,[§] Jae Heung Lim,[§] Seok Hyang Kim,[§] Honggu Chun,[∥] Eunhye Kim,[†] and Young June Park[†,§,*]

[†]NANO Systems Institute (NSI), Seoul National University, Seoul 151-742, Korea, [‡]Technology Commercialization Division-SMEs Cooperation Center, ETRI, Daejeon 305-700, Korea, [§]School of Electrical Engineering, Seoul National University, Seoul 151-742, Korea, and [∥]Department of Biomedical Engineering, Korea University, Seoul 136-703, Korea. [⊥]These authors contributed equally to this work.

ABSTRACT A novel electrical DNA biosensor is presented, which consists of gold (Au) nanoscale islands and a single-walled carbon nanotube (SWCNT) network on top of a concentric Au electrode array (also referred to as the CGi). The decorated Au islands on the SWCNT network provide ideal docking sites for ss-DNA probe (p-DNA) molecules. They also provide better adhesion between the SWCNT network and the chip substrate. In addition, the concentric electrode gives asymmetric current voltage characteristics in the solution and provides more flexible bias options to the electrodes. The sensor system is applied to a DNA sensor after functionalization with a 25mer p-DNA (5′-HSC_6-C_{18}-GCCATTCTCACCGGATTCAGTCGTC-3′), hereafter called the [CGi+p-DNA]. The response of the DNA sensor has been measured in both real-time during hybridization with the complementary target ss-DNAs (t-DNA) and the static mode after the hybridization and washing steps. A wide dynamic range from the 100 fM to 1 μM has been achieved from the real-time mode and the static mode. Moreover, it is shown that the sensor system differentiates partially mismatched (single nucleotide polymorphism (SNP), half mismatch, noncomplementary) t-DNA, as well. The [CGi] sensor platform can be easily extended to target specific biological recognition elements such as aptamers or proteins.

KEYWORDS: single-walled carbon nanotube · CNT FET · electrical biosensor · DNA sensor · gold islands · SNP · dynamic range · random network

Electrical biosensors provide an attractive alternative in gathering information from biological samples through electrical signals. There have been a number of approaches to achieve the electrical sensor based on various nanomaterials such as the single-walled (SW) carbon nanotube (CNT), multi-walled (MW) CNT, and silicon nanowire (SiNW) for DNA or other biomolecular detection.[1−10] Among them, the CNT-based sensors have been considered to be the most promising candidate for label-free detection of biomolecules due to their high sensitivity, small size, high mechanical strength, and stability in harsh chemical environments[1−8] when compared to the biosensors adopting other materials such as SiNW sensors.[9,10] However, despite great advances in the field of nanostructure materials and devices, there has been minimal impact on the application and commercialization of biosensors based on the electrical sensing. Key factors impeding the applications of the technology are difficulties in having reliable and sensitive platforms and difficulties in integrating the sensor to the signal processing CMOS chip, which are necessary to compete with the well-established conventional optical chip technology. For instance, the CNT-based sensor approaches require high-temperature processes to grow the CNTs and to remove unwanted metal catalysts. Also, in case of the SiNW-based sensors, etching of the unwanted silicon area and surface treatment of silicon require complicated and high-temperature processes, which make the integration to the CMOS chip difficult.

We propose a sensor array platform, [CGi], a gold (Au) island-coated SWCNT network as an electrical channel connecting two Au electrodes having the concentric structure (Scheme 1 and Figure 1) to overcome the above fabrication problems of CNT- and SiNW-based sensors especially in integration to the CMOS chips.[11] We briefly summarize two salient features of the sensor platform due to the concentric electrode structures. First, an additional reference electrode is not needed to stabilize the solution electrostatic potential because the electrostatic potential of the solution is determined by the potential applied to the enclosed electrode which has much larger area. Furthermore, the asymmetrical nature of this biasing system provides more flexible biasing options, showing higher sensitivity results from the "self-gating effect" created by the concentric electrode structure. This self-gating phenomenon has been recently published by our group.[12,13] Second, the [CGi] channel consisting of the SWCNT network and Au nanoislands between the electrodes can be fabricated by SWCNT dip-coating and physical evaporation of Au, respectively. Thanks to the concentric electrode structure, as shown in Scheme 1 and Figure 1,

* Address correspondence to ypark@snu.ac.kr.

Received for review October 31, 2010 and accepted April 11, 2011.

Published online April 11, 2011
10.1021/nn102938h

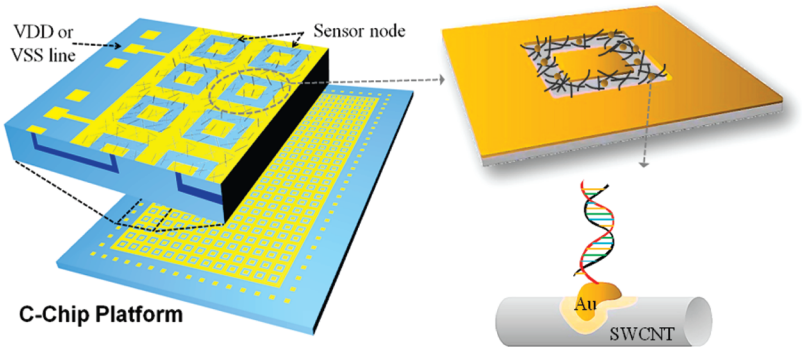

Scheme 1. Schematic diagram of the chip structure including an array of the concentric electrode and DNA sensing of [CGi] platform.

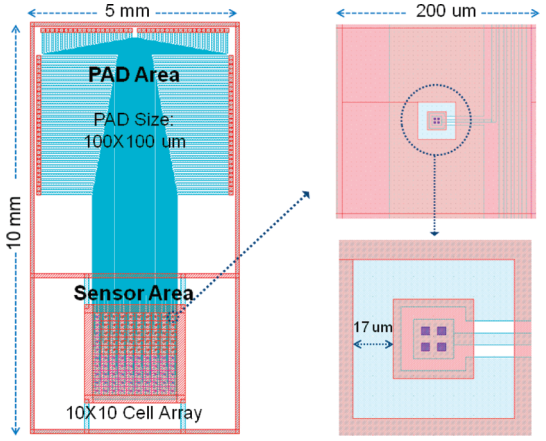

Figure 1. Concentric structures of the chip. The distance between the central and surrounding electrode is 17 μm.

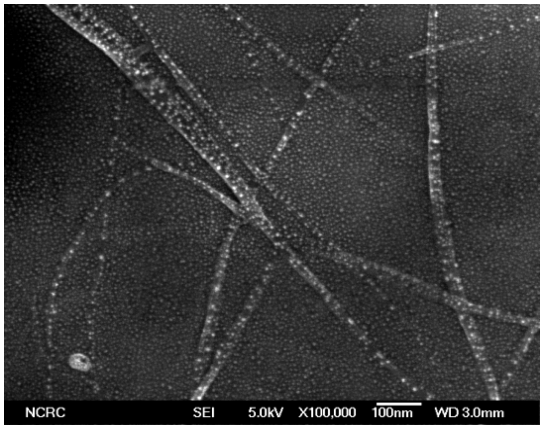

Figure 2. FE-SEM image of the channel area (TEOS layer) of the [CGi] system. The SWCNT network decorated with Au nanoparticles is integrated between the electrodes. They are randomly distributed on the oxide substrate to form a channel. The white dots indicate Au islands, which are the docking places for the p-DNA molecules.

unwanted CNTs coated on the enclosing electrode do not have to be removed because the enclosing electrode effectively shields the interference from the neighbor channel device. The two features make the integration of the channel to the CMOS chip having the signal processing circuits easy and reliable. The decorated Au nanoparticles on the SWCNT network can be used as a substrate or a linker for biomolecular sensor application by attaching probe molecules with thiol functional groups. They also provide better adhesion between the SWCNT network and the chip substrate.

In this paper, we applied our sensor platform to the DNA sensing and report the sensitivity, specificity, and stability measurements. When the target ss-DNA (t-DNA) molecules are applied to the [CGi+p-DNA] sensor, hybridization occurs on both the source/drain electrode and the Au islands. The hybridization events modify the Au work function in the electrode−SWCNT region and the Au islands in the channel region, increasing the contact resistance and channel resistance, respectively. The response of the sensor system to the target DNAs was monitored both by the real-time mode and by the static mode. In the static mode, the measurement has been conducted in an ideal deionized water condition after hybridization and washing steps. The results demonstrate that label-free detection of t-DNA down to the 100 fM range with wide dynamic range is possible from both measurement modes. This technique with such a wide dynamic range of real-time electrical measurements and the static mode has not been previously demonstrated to the best of our knowledge.

RESULTS AND DISCUSSION

Characteristics of the [CGi]. The [CGi] device was constructed by decorating the SWCNT network with Au nanoparticles on top of an array of the concentric Au electrodes. The Au particles were deposited to enhance the attachment of the SWCNT network to the electrodes and to provide a docking place for the probe molecules. The FE-SEM analysis showed that the SWCNT network was distributed randomly on the oxide substrate, and Au particles around 3 nm in diameter were randomly distributed on the SWCNT network as well as the underlying tetraethylorthosilicate (TEOS) layer, forming networked resistors between electrodes (Figure 2). The measured resistances of the Au decorated devices ([CGi], average: ~1.0 KΩ) were reduced by half compared to that of the

bare SWCNT network devices ([CNN], average: ~2.0 KΩ). The stability of [CGi] was better than the bare [CNN] system because the Au islands were attached not only to the SWCNT network but also to the substrate, thereby strengthening the attachment force between the SWCNT network and the SiO_2 substrate. Without the Au islands, the SWCNT network is stacked on the substrate by weak van der Waals forces and easily detached by mechanical stress during field operation of the chip. [CGi] showed stable electrical characteristics compared to [CNN] as follows: (i) 12 [CGi] samples have been exposed to air for 2 days, and the change of the resistance has been observed. It has been found that initial resistance (R) of 721 ± 45 Ω has been changed to R of 738 ± 48 KΩ after 2 days. In comparison, the CNN samples showed the change in the distribution of the resistance from 2.11 ± 0.55 to 3.39 ± 2.60 KΩ after 1 day and R of 3.89 ± 2.96 KΩ after 6 days. (ii) After applying a constant voltage (−0.3 V), to two samples for 1800 s, the currents were changed from −432 to −428 μA and from −417 to −413 μA, whereas the [CNN] samples changed from −145 to −147 μA and from −248 to −257 μA (Figure S1 in Supporting Information). Moreover, the nonspecific binding between SWCNTs and the biomolecules can be avoided by the Au islands. This is because the gap between Au nanoparticles is so narrow (~10 nm) that unwanted molecules have less chance of touching the SWCNT network.

The [CGi] was functionalized with a thiolated 25mer p-DNA molecule *via* the Au−S bond. The thiol groups in the p-DNAs were linked to the Au islands (Scheme 1). Real-time current measurements of the p-DNA immobilization are shown in Figure 3a (for further details, see Figure S2a in the Supporting Information). The change in current after the immobilization of 1200 s, $\Delta I_{p\text{-}DNA}/I_{TE}$, was −34%. The immobilized p-DNA sample, [CGi+p-DNA], was washed with TE buffer and deionized water followed by a drying process with N_2. The current of [CGi+p-DNA] after immobilization and wash-and-dry process showed a decrease in current by ~40% from the pristine [CGi] in the air (Figure 3a). We then applied buffer solutions for the t-DNA sensing experiment and monitored the change in current. Eight samples of [CGi+p-DNA] with the resistance distribution of 1.31 ± 0.28 KΩ decreased the current levels after applying TE buffer. It is encouraging to notice that the rate of the current decrease is tightly distributed regardless of the initial distribution of the sample, 1.315 ± 0.395 KΩ; after 400 s, $\Delta I_{TE}/I_{air}$ was −68.6 ± 2.8%; after 800 s, $\Delta I_{TE}/I_{air}$ was −73.0 ± 1.4%; and after 1200 s, $\Delta I_{TE}/I_{air}$ was −74.6 ± 1.1% (Figure S2b in Supporting Information and Figure 3a). Also, addition of human serum to two samples of [CGi+p-DNA] with an average R of 1.43 ± 0.09 KΩ resulted in a current change with the same ratio (after 400 s, $\Delta I_{TE}/I_{air}$ was −61.9 ± 0.8%; after 800 s, $\Delta I_{TE}/I_{air}$ was −64.9 ± 0.2%; after 1200 s, $\Delta I_{TE}/I_{air}$ was −66.4 ± 0.1%) in the air (Figure 5a).

Real-Time Electrical Measurement in TE Buffer. The [CGi+p-DNA] devices have been used to detect the concentrations of target analytes consisting of matched and mismatched t-DNAs. In Figure 3b, the real-time responses of the [CGi+p-DNA] devices to the mismatched t-DNAs (SNP, half mismatch, noncomplementary) with a fixed concentration of 33 μM at −0.3 V are shown, and the specificity determined at +0.3 V is shown in Figure S4 (Supporting Information). When a t-DNA droplet was introduced, the electrical current rapidly decreased. In contrast, upon addition of the TE buffer without t-DNA as a control, the devices showed a slight decrease in the current. The ratios of the current decreases of the noncomplementary t-DNA and half matched t-DNA, compared to that of the complementary t-DNA, are about a ~53 and ~84% decrease, respectively. The salient differences in the sensitivity between the complementary and SNP t-DNA can be explained by two factors. The binding affinity is larger in the case of complementary t-DNA compared with that of the SNP t-DNA, so that total hybridized events are large in number for the complementary t-DNA case. At the same time, the melting temperatures (T_m) of the hybridized DNAs, which are not much different for two cases of the hybridization in the analytes, tend to decrease to room temperature in the surface binding events such as with the gold particles.[14] Difference in the kinetic parameters[15,16] and the reduction of the melting temperature of the SNP and half matched t-DNAs contribute to the differentiation from the t-DNA samples. Shown in Figure 3c is the different response of the sensors to complementary or noncomplementary t-DNAs with two different concentrations, 3.3 and 33 μM. Another set of experiments was conducted to determine the sensitivity of [CGi+p-DNA] by sequential t-DNA injections with increasing 10 times of the t-DNA concentration from 2 fM (Figure 3d,e). As expected, the sensitivity of [CGi+p-DNA], $\Delta I_{t\text{-}DNA}/I_{p\text{-}DNA}$ (%), increased as the concentration of the complementary t-DNA increased. Moreover, the sensor device showed sensitivity for a wide range of t-DNA concentration (100 fM to 1 μM) with the limit of detection (LOD) of about 100 fM. The device current was measured by the constant voltage mode at −0.3 V (Figure 3d) and +0.3 V (Figure 3e). The experimental device (t-DNA) and the control device (TE buffer) were measured simultaneously to avoid variations among the sample devices and the experimental environments. Because the t-DNAs from previous experiments were not removed for the next experiment, the measured curves show a continuously increasing or decreasing trend depending on the applied voltage (Figure 3d,e). However, since the t-DNA is added right after the start of the electrical measurement (power on), the measured curves for each concentration show transient responses in the early stage. It can be observed that the response time is relatively uniform for different concentration and shorter than the time expected by the Langmuir type adsorption theory. We

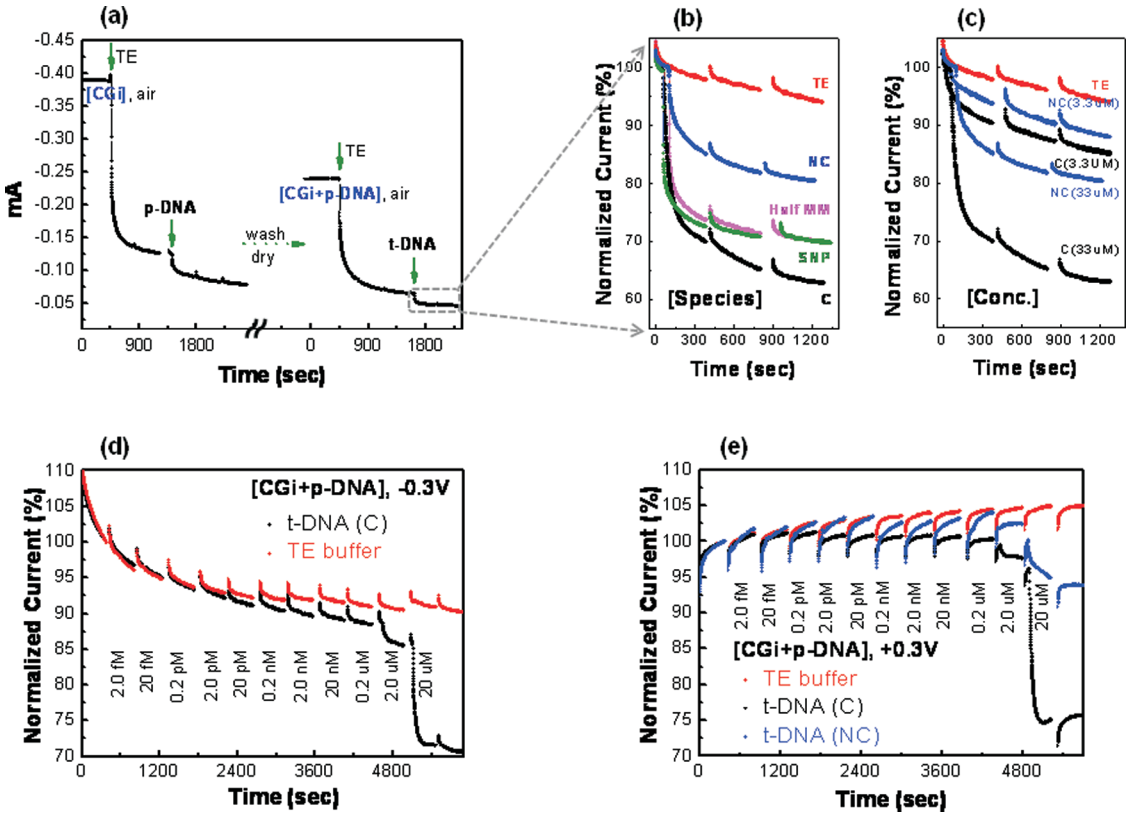

Figure 3. (a) Real-time response of the [CGi+p-DNA] device after applying TE buffer, p-DNA for immobilization, TE buffer after wash-and-dry process, and t-DNA for hybridization. Real-time response to different t-DNA samples of (b) 33 μM and (c) 3.3 μM and 33 μM to check the specificity. Real-time response after a sequence application of t-DNAs by increasing the concentration by 10 times. The current was measured by a constant voltage mode at −0.3 V (d) and +0.3 V (e). The response to the TE buffer only without t-DNA is also monitored as a control. C, complementary; NC, noncomplementary; MM, mismatch; SNP, single nucleotide polymorphism.

presume that the short time constant partly stems from the limited volume of a droplet used in our experiment. When a limited volume droplet size is used, the t-DNA concentration reduces as the t-DNA is adsorbed because the t-DNA number should be conserved. We have performed a simulation to see the effects of the droplet size and t-DNA concentration as shown in the Figure S6 (Supporting Information). It was found that the time constant for the droplet size of 80 μL is much shorter (about 10 times) than the time constant for the droplet of infinite size. Also, the simulated time response of the adsorption for different concentration of t-DNA is shown in the Figure S7 (Supporting Information). It should be noted that the responses are almost identical for the concentrations less than 10 nM, while the response time becomes shorter as the concentration becomes higher. It is interesting to see that the total number of t-DNA in the 10 nM droplet is almost the same as the total number of p-DNA in the surface. The responses of the noncomplementary t-DNA were compared with those of the complementary t-DNA in Figure 3e. The saturated currents of the noncomplementary t-DNA approach those of the control buffer for concentrations of t-DNA less than 20 pM, implying that the nonspecific binding effect is almost negligible for t-DNA under 20 pM. On the other hand, the responses of the noncomplementary t-DNA higher than 20 pM are slower and do not approach the saturation currents of the control buffer. From the observation, we can guess that, when the noncomplementary t-DNA concentration exceeds some concentration, the influence of the nonspecific binding cannot be ignored even though the response is smaller than that of the complementary t-DNA. So, there is a necessity to do a washing process to determine how much nonspecific binding is involved for this measurement.

Figure 4a summarizes the sensitivity data *versus* t-DNA concentration measured for two different applied biases: −0.3 V and +0.3 V. A slight better sensitivity is obtained for the bias of +0.3 V and can be explained by the different device operation modes caused by the asymmetrically shaped electrodes.[12] It is interesting to see that the dynamic range is the 7 orders of concentration, from 100 fM to 1 μM, with the LOD of ~100 fM. Considering that the total number of t-DNA molecules in the droplet is on the order of $\sim 5 \times 10^6$ for the case of 100 fM, it is striking to see the sensitivity in such a low concentration. In order to observe the sensing behavior of the [CGi+p-DNA] in a more realistic environment, similar experiments have been performed in serum (Figure 5). As the control experiment, the serum solution

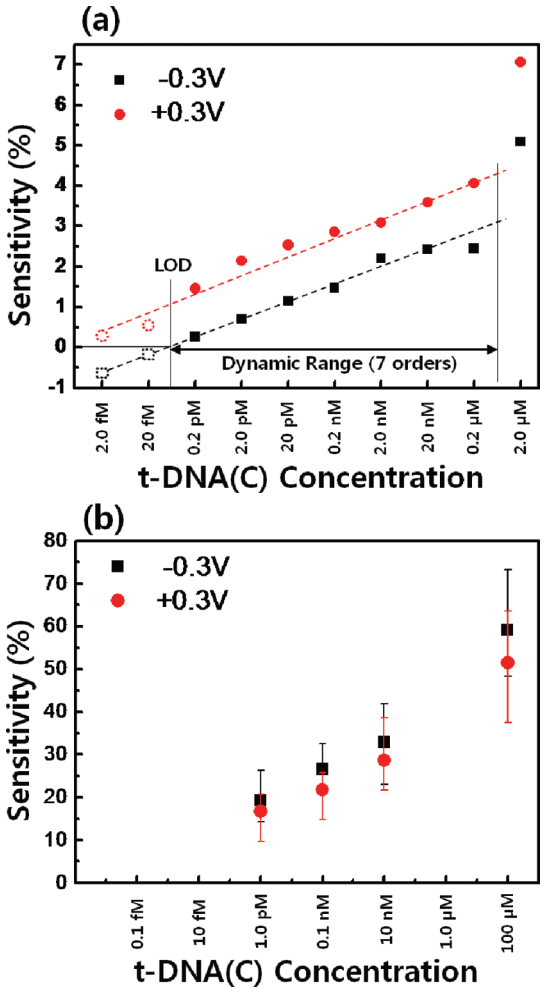

Figure 4. Sensitivity of the [CGi+p-DNA] as the function of t-DNA concentration for two different measurement conditions. (a) Real-time measurements conducted at ~400 s after application of t-DNAs in the TE buffer solution. The response to the TE buffer only without t-DNA is also monitored as a control. The sensitivity is defined as the difference in the normalized current with and without the t-DNA hybridization (sensitivity = $(\Delta I_{t\text{-}DNA} - \Delta I_{TE})/I_{p\text{-}DNA}$, %). (b) Sensitivity of measurements conducted after overnight hybridization and washing process in the deionized water. The sensitivity is determined by the difference in the current before and after the t-DNA hybridization without control devices (sensitivity = $\Delta I_{t\text{-}DNA}/I_{p\text{-}DNA}$, %).

without t-DNA has been applied. As shown in Figure 5b, there is not much difference in slope between the serum and the TE buffer condition. Once the TE droplet including the t-DNA is applied to the solution, the sensor shows the time response as the t-DNA reaches the surface-bound p-DNA with the specific diffusivity and hybridizes with the p-DNA following the specific hybridization kinetics. Compared with the case of the TE buffer solution, the serum solution shows much slower response time. There may be two reasons; one is due to the lower diffusion constant of the t-DNA in the serum solution as much as the half[17] and the other may be the contribution of the nonspecific adsorption of various kinds of protein contained in the serum.[18] Accordingly, the specific DNA hybridization kinetics in serum may be reduced to slow down the response time.

Measurements after the Washing Step. In addition to the time measurements, electrical measurements (sweep mode, −0.3 V ~ +0.3 V) were also performed after overnight hybridization and washing process. In this case, the electrical measurements can be conducted in ideal solution environments, deionized water at room temperature. Hereafter, the measurement will be called the "static" measurement. Figure 4b and Figure S5 (Supporting Information) show the sensitivity for a wide range of concentrations of the complementary t-DNA. More sensitive values (sensitivity = $\Delta I_{t\text{-}DNA}/I_{p\text{-}DNA}$, %) are obtained compared with the real-time measurements explained above. It is attributed to the removal of nonspecific binding of the t-DNA during the washing step and the mitigation of the charge screening effect. In addition, the modulation of the Au work function due to the DNA hybridization gives more effective channel conductance reduction in the deionized water. More detailed explanation for the sensing mechanism will be found in the next section. Figure S5b (Supporting Information) shows the specificity of the [CGi+p-DNA] sensor devices among complementary, half mismatch, and the SNP t-DNA after the washing step at −0.3 V and +0.3 V.

Sensing Mechanism. It is known that DNA immobilization and hybridization on Au electrodes result in a change in the Au work function locally. In recent reports, the sensing mechanisms of the DNA sensors based on CNTs have been explained by the modulation of the current due to a shift in the energy alignment between the Au contact and CNT.[19−23] In our sensor device, the DNA immobilization and hybridization occur both on the Au islands and the source/drain electrodes. The DNA immobilization of p-DNA and hybridization with t-DNA on the Au electrode reduce the Au work function and increase the Schottky barrier, increasing the contact resistance as schematically shown in Figure 6. On the other hand, the hybridization on the Au island reduces the channel conductance due to hole carrier depletion around the Au island. Consequently, DNA hybridization on both the electrode contact and the Au islands in the channel area contributes to the reduction of the overall conductance.

For the reason of sensitivity for a wide range of target concentrations, we may refer the reports on the relation between the dynamic range and the complexity of the nanostructuring.[24,25] Since our devices have the Au nanoparticles with various sizes determined by the random level of agglomeration during Au deposition, as shown in the SEM picture in Figure S8 (Supporting Information) and Figure 2, the wide dynamic range obtained in the [CGi] device can be explained in a similar manner. If we assume that the amount of change in the work function of the Au islands is related to the size of the Au particles on the SWCNT for each t-DNA hybridization and there is a difference in the number of attached p-DNAs according

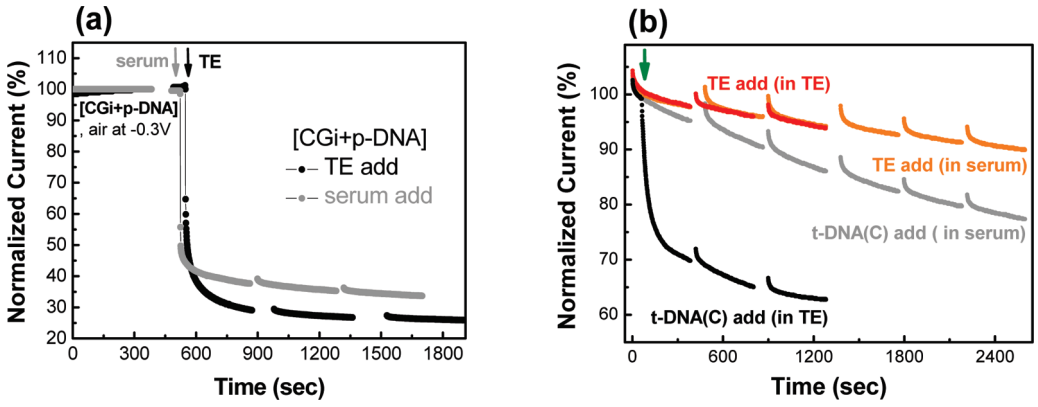

Figure 5. (a) Real-time response of the [CGi+p-DNA] device after adding TE buffer and human serum. The current level is normalized to the current measured in the air. (b) Real-time response after applying TE droplets including complementary t-DNAs to the [CGi+p-DNA] devices in TE buffer and human serum solutions at −0.3 V. TE-only droplets are also applied as control. Complementary t-DNA solution (33 μM, 8 μL) and TE buffer (8 μL) were added to 15 μL of TE buffer (black and orange) and to 15 μL of human serum (gray and brown), respectively.

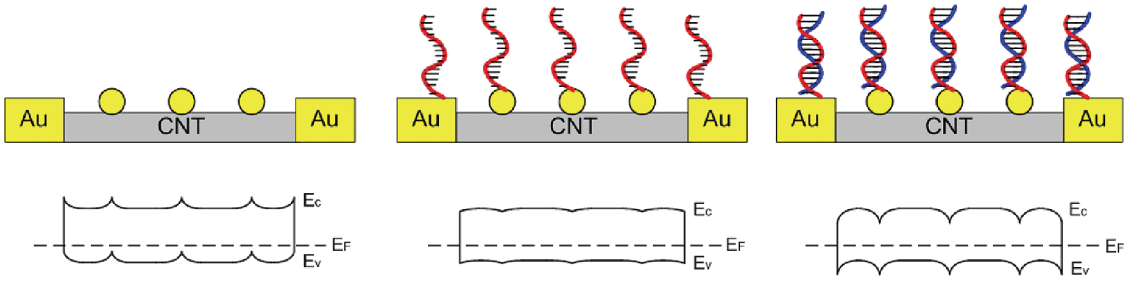

Figure 6. Schematics and corresponding energy band diagrams of the [CGi] system. The work function of Au is decreased by DNA. (a) Bare [CGi]: hole carriers are accumulated by the Au nanoparticles (work function of Au = 5.1 eV, work function of SWCNT = ~5.0 eV). (b) After immobilization of p-DNA: as the probe DNA is immobilized, the Schottky barrier increases and the hole carriers are depleted. (c) Hybridization of t-DNA: after the hybridization, the electrical conductance in the contact and the channel area decreases due to the reduction of Au work function.

TABLE 1. DNA Sequences Used in the Experiments

	ss-DNA	sequences
	probe	5′-HSC_6-C_{18}-GCCATTCTCACCGGATTCAGTCGTC-3′
target	complementary	3′-CGGTAAGAGTGGCCTAAGTCAGCAG-5′
target	SNP	3′-CGGTAAGAGTGG**G**CTAAGTCAGCAG-5′
target	half mismatch	3′-CGGTAAGAGTGG**GGATTCAGTCGTC**-5′
target	noncomplementary	3′-**GCCATTCTCACCGGATTCAGTCGTC**-5′

to the size of Au particles, the smaller particles can give a carrier depletion effect to CNT even at very low t-DNA concentrations while the larger particles tend to respond only when the majority of the p-DNAs are hybridized with the t-DNAs. In this way, the sensor can respond to a wide range of target DNA concentration. We are planning experiments with different sized Au particles to further verify the model as a future study.

CONCLUSIONS

We have proposed a sensor platform based on the [CGi] for label-free DNA detection and shown that the device shows a wide dynamic range with a 7 order dynamic range. With the [CGi+p-DNA] device immobilized with a 25mer p-DNA, we have conducted two experiments; real-time measurement during the hybridization events and the more ideal measurement after the hybridization and washing steps. Both experiments show a high binding affinity with the complementary t-DNA targets from 100 fM to 1 μM range. In addition, a reasonable specificity between complementary and noncomplementary t-DNAs has been observed at very small concentrations of t-DNA even in the real-time measurement. The sensor platform may be used to the label-free detection of the unknown DNA samples in real-time and expanded to detection of other biomolecules, such as protein.

METHODS

Materials. All chemicals and solvents used in these experiments were of reagent grade and used without further purification. The HPLC grade single-stranded DNA samples were purchased from Bioneer (Korea). The details are shown in Table 1. The purification and coating of the SWCNT (ASP-100F

produced by Il-jin Nanotech, Korea) were done according to the previously reported procedures.[11,26] By boiling the SWCNTs in HNO_3, contaminants were removed, and functional groups such as carboxylic acid, hydroxyl, and carbonyl groups were intentionally formed at the surfaces of the SWCNTs. This induced a good dispersion in the coating solvent and adhesion on the hydrophilic thick TEOS layer. Afterward, to make the SWCNT coating solution, the SWCNTs were dispersed in 1, 2-dichlorobenzene with a concentration of 0.10 mg/mL, and ultrasonication was performed for 20 h. The surface morphology of the sample was evaluated with an optical microscope and field emission scanning electron microscopy (FE-SEM).

Preparation of the [CGi+p-DNA] Samples. The test chips having a concentric electrode structure (Figure 1) were fabricated at the Interuniversity Semiconductor Research Center (ISRC) of Seoul National University using a two-metal process which consisted of aluminum as the first metal and Au as the second metal. On a thermally oxidized Si wafer, the first metal routing patterns were formed using conventional lithography and etching processes.[11,13] Afterward, a 10 000 Å thick TEOS oxide film was deposited and via contacts were formed. The substrate was evaporated and patterned to form a 4000 Å concentric Au electrode using the lift-off method.

Using the SWCNT coating solution, the chips were coated with the SWCNT layer by dipping for 30 s and withdrawing at a velocity of 3 mm/min. Thereafter, 1 nm thick Au nanoparticles were deposited on the SWCNT network using a thermal evaporator, which resulted in the formation of a random sized Au particle layer on the SWCNT network by annealing at 300 °C for 30 min.

To immobilize the p-DNA molecules for sensing of specific target molecules, bare [CGi] samples were immersed in 100 μM (10 μL) of p-DNA solution (Tris-EDTA buffer, pH 7.6) for 12 h at room temperature and rinsed several times with TE buffer and deionized water.

Real-Time Electrical Measurements for t-DNA Sensing. The device current was measured at a constant voltage of −0.3 V or +0.3 V between the central electrode and grounded surrounding electrode in TE buffer solution. The equipment we used for the measurements was Agilent 4145B. Because of the restrictions imposed by the measuring equipment, a limited number of data points could only be collected, and power had to be newly applied for each and every measurement. Every measurement was done in a time period less than 400 s after the t-DNA was introduced. Figures 3 and 5 show noncontinuous curves even though there was no time delay after each measurement. The sensitivity and specificity were measured in real-time at room temperature after adding the target analytes in TE buffer solution without using any washing step, varying the t-DNA concentration and species. To evaluate the measured results more accurately, other control electrodes were also measured simultaneously without any t-DNA in the sample using the same chip.

Static Electrical Measurements after Washing Steps for t-DNA Sensing. For the static measurement, the chips have been through the overnight hybridization and washed by two-step processes. First, after hybridization, the chip was diluted by a large amount of TE buffer solution followed by washing in the deionized water. After fully drying the chips at room temperature, we applied the deionized water and started the static measurement after the chips were stabilized in the deionized solution for 20 min. The device current was measured by sweeping the voltage from −0.3 V to +0.3 V. The sensitivity was determined by the difference in the current before and after the t-DNA hybridization.

Acknowledgment. This work was supported by the BK21 Program, the Nano System Institute National Core Research Center (NSI-NCRC) program of KOSEF, and the Industrial Source Technology Development program (10033590) of the Ministry of Knowledge Economy (MKE), Korea. We appreciate useful discussions with Dr. Yang Liu and Prof. Robert W. Dutton of Stanford University. We also thank Jae-Hoon Lee of Digital Genomics Inc. for experimental support.

Supporting Information Available: More figures and details of the stability of the [CGi] chips (in air at −0.3 V), real-time specificity (in TE buffer at +0.3 V) of [CGi+p-DNA], the measurement results after the washing step, and the simulation results of volume limited t-DNA hybridization are available. This material is available free of charge *via* the Internet at http://pubs.acs.org.

REFERENCES AND NOTES

1. Yang, W.; Thordarson, P.; Gooding, J. J.; Ringer, S. P.; Braet, F. Carbon Nanotubes for Biological and Biomedical Applications. *Nanotechnology* **2007,** *18*, 412001–412013.
2. Kong, J.; Franklin, N. R.; Zhou, C.; Chapline, M. G.; Peng, S.; Cho, K.; Dai, H. Nanotube Molecular Wires as Chemical Sensors. *Science* **2000,** *287*, 622–655.
3. Postma, H. W. C.; Teepen, T.; Yao, Z.; Grifoni, M.; Dekker, C. Carbon Nanotube Single-Electron Transistors at Room Temperature. *Science* **2001,** *293*, 76–79.
4. Balasubramanian, K.; Burghard, M. Biosensors Based on Carbon Nanotubes. *Anal. Bioanal. Chem.* **2006,** *385*, 452–468.
5. Katz, E.; Willner, I. Biomolecule-Functionalized Carbon Nanotubes: Applications in Nanobioelectronics. *ChemPhysChem* **2004,** *5*, 1084–1104.
6. Allen, B. L.; Kichambare, P. D.; Star, A. Carbon Nanotube Field-Effect-Transistor-Based Biosensors. *Adv. Mater.* **2007,** *19*, 1439–1451.
7. Gruner, G. Carbon Nanotube Transistors for Biosensing Applications. *Anal. Bioanal. Chem.* **2006,** *384*, 322–335.
8. Lee, B. Y.; Seo, S. M.; Lee, D. J.; Lee, M.; Lee, J.; Cheon, J.-H.; Cho, E.; Lee, H.; Chung, I.-Y.; Park, Y. J.; *et al.* Biosensor *System-on-a-Chip* Including CMOS-Based Signal Processing Circuits and 64 Carbon Nanotube-Based Sensors for the Detection of a Neurotransmitter. *Lab Chip* **2010,** *10*, 894–898.
9. Zheng, G.; Patolsky, F.; Cui, Y.; Wang, W. U.; Lieber, C. M. Multiplexed Electrical Detection of Cancer Markers with Nanowires Sensor Array. *Nat. Biotechnol.* **2005,** *23*, 1294–1301.
10. Li, Z.; Chen, Y.; Li, X.; Kamins, T. I.; Nauka, K.; Williams, R. S. Sequence-Specific Label-Free DNA Sensors Based on Silicon Nanowires. *Nano Lett.* **2004,** *4*, 245–247.
11. Ko, J. W.; Koo, H. C.; Kim, D. W.; Seo, S. M.; Kang, T. J.; Kwon, Y.; Yoon, J. L.; Cheon, J. H.; Kim, Y. H.; Kim, J. J.; *et al.* Electroless Gold Plating on Aluminum Patterned Chips for CMOS-Based Sensor Applications. *J. Electrochem. Soc.* **2009,** *157*, D46–D49.
12. Kim, D. W.; Choe, G. S.; Seo, S. M.; Cheon, J. H.; Kim, H.; Ko, J. W.; Chung, I. Y.; Park, Y. J. Self-Gating Effects in Carbon Nanotube Network Based Liquid Gate Field Effect Transistors. *Appl. Phys. Lett.* **2008,** *93*, 243115(1−3).
13. Cheon, J. H.; Lim, J. H.; Seo, S. M.; Woo, J.-M.; Kim, S. H.; Kwon, Y.; Ko, J. W.; Kang, T. J.; Kim, Y. H.; Park, Y. J. Electrical Characteristics of the Concentric-Shape Carbon Nanotube Network Device in pH Buffer Solution. *IEEE Trans. Electron Devices* **2010,** *57*, 2684–2689.
14. SantaLucia, J. A Unified View of Polymer, Dumbbell, and Oligonucleotide DNA Nearest-Neighbor Thermodynamics. *Proc. Natl. Acad. Sci. U.S.A.* **1998,** *95*, 1460–1465.
15. Harris, N. C.; Kiang, C.-H. Defects Can Increase the Melting Temperature of DNA−Nanoparticle Assemblies. *J. Phys. Chem. B.* **2006,** *110*, 16393–16396.
16. Peterlinz, K. A.; Georgiadis, R. M.; Herne, T. M.; Tarlov, M. J. Observation of Hybridization and Dehybridization of Thiol-Tethered DNA Using Two-Color Surface Plasmon Resonance Spectroscopy. *J. Am. Chem. Soc.* **1997,** *19*, 3401–3402.
17. Rosenson, R. S.; McCormick, A.; Uretz, E. F. Distribution of Blood Viscosity Values and Biochemical Correlates in Healthy Adults. *Clin. Chem.* **1996,** *42*, 1189–1195.
18. Gong, P.; Lee, C.-Y; Gamble, L. J.; Castner, D. G.; Grainger, D. W. Hybridization Behavior of Mixed DNA/Alkylthiol Monolayers on Gold: Characterization by Surface Plasmon Resonance and ^{32}P Radiometric Assay. *Anal. Chem.* **2006,** *78*, 3326–3334.

19. Heller, I.; Janssens, A. M.; Mannik, J.; Minot, E. D.; Lemay, S. G.; Dekker, C. Identifying the Mechanism of Biosensing with Carbon Nanotube Transistors. *Nano Lett.* **2008,** *8*, 591–595.
20. Gui, E. L.; Li, L.-J.; Zhang, K.; Xu, Y.; Dong, X.; Ho, X.; Lee, P. S.; Kasim, J.; Shen, Z. X.; Rogers, J. A. DNA Sensing by Field-Effect Transistors Based on Networks of Carbon Nanotubes. *J. Am. Chem. Soc.* **2007,** *129*, 14427–14432.
21. Tang, X.; Bansaruntip, S.; Nakayama, N.; Yenilmez, E.; Chang, Y.-l.; Wang, Q. Carbon Nanotube DNA Sensor and Sensing Mechanism. *Nano Lett.* **2006,** *6*, 1632–1636.
22. Gui, E. L.; Li, L. J.; Lee, P. S.; Lohani, A.; Mhaisalkar, S. G.; Cao, Q.; Kang, K.; Rogers, J. A.; Tansil, N. C.; Gao, Z. Electrical Detection of Hybridization and Threading Intercalation of Deoxyribonucleic Acid Using Carbon Nanotube Network Field-Effect Transistors. *Appl. Phys. Lett.* **2006,** *89*, 232104(1−3).
23. Arinaga, K.; Rant, U.; Tornow, M.; Fujita, S.; Abstreiter, G.; Yokoyama, N. The Role of Surface Charging during the Coadsorption of Mercaptohexanol to DNA Layers on Gold: Direct Observation of Desorption and Layer Reorientation. *Langmuir* **2006,** *22*, 5560–5562.
24. Soleymani, L.; Fang, Z.; Sargent, E. H.; Kelley, S. O. Programming the Detection Limits of Biosensors through Controlled Nanostructuring. *Nat. Nanotechnol.* **2009,** *4*, 844–848.
25. Gasparac, R.; Taft, B. J.; Lapierre-Devlin, M. A.; Lazareck, A. D.; Xu, J. M.; Kelley, S. O. Ultrasensitive Electrocatalytic DNA Detection at Two-and Three-Dimensional Nanoelectrodes. *J. Am. Chem. Soc.* **2004,** *126*, 12270–12271.
26. Jang, E. Y.; Kang, T. J.; Im, H. W.; Kim, D. W.; Kim, Y. H. Single-Walled Carbon-Nanotube Networks on Large-Area Glass Substrate by the Dip-Coating Method. *Small* **2008,** *4*, 2255–2261.